Emergence of spatially extended pair coherence through incoherent local environmental coupling

Jean-Sébastien Bernier, Peter Barmettler, Dario Poletti, and Corinna Kollath

Phys. Rev. A **87**, 063608 — Published 10 June 2013

DOI: 10.1103/PhysRevA.87.063608

Emergence of spatially extended pair coherence through incoherent local environmental coupling

Jean-Sébastien Bernier,[1] Peter Barmettler,[2] Dario Poletti,[3] and Corinna Kollath[2,4]

[1] *Department of Physics and Astronomy, University of British Columbia, Vancouver V6T 1Z1, Canada.*
[2] *Département de Physique Théorique, Université de Genève, CH-1211 Genève, Switzerland.*
[3] *Singapore University of Technology and Design, 20 Dover Drive, 138682 Singapore.*
[4] *University of Bonn, HISKP, Nussallee 14-16, 53115 Bonn, Germany*

We demonstrate that quantum coherence can be generated by the interplay of coupling to an incoherent environment and kinetic processes. This joint effect even occurs in a repulsively interacting fermionic system initially prepared in an incoherent Mott insulating state. In this case, coupling a dissipative noise field to the local spin density produces coherent pairs of fermions. The generated pair coherence, while metastable, is long lived and spatially extended. This conceptually surprising approach provides a novel path towards a better control of quantum many-body correlations.

PACS numbers: 03.65.Yz, 05.30.Fk, 67.85.-d

I. INTRODUCTION

In recent years, various experimental methods have been developed to dynamically generate non-trivial correlations in quantum materials. On the one hand, external electromagnetic fields have been used to photo-induce phase transitions in solid state materials [1]. For example, spin density wave order was induced in the normal state of a pnictide compound using femtosecond optical pulses [2]. A Josephson plasmon, typically present in a superconducting state, has even been triggered in a non-superconducting striped-order cuprate by the application of mid-infrared femtosecond pulses [3]. On the other hand, environmental tailoring [4] has been used to prepare highly entangled states such as a Bell state of two ions [5] or a Tonks-Giradeau-like state in a molecular quantum gas [6]. In these examples, the realization of complex states relies on the same principle as optical pumping whereby atoms are prepared in so-called dark states immune to environmental coupling.

We report on a complementary mechanism where dynamical generation of coherence is achieved through the combined effect of a simple local dissipative coupling and kinetic processes. To examplify the inner workings of this mechanism, we consider an ultracold fermionic gas in an optical lattice subjected to local spin-polarization measurements carried out by phase-contrast imaging [7] or spatial and temporal light field fluctuations. The dissipative coupling heats up the system and destroys single-particle correlations. At the same time the number of local pairs, which are immune to the dissipative coupling, increase due to kinetic hopping. Unexpectedly, these local pairs then act as a source for the generation of pair correlations over longer distances. The produced correlations, while metastable, are long lived and reminiscent to those of the celebrated η-pairing state [8, 9], a condensate of bound on-site pairs of momentum $k = \frac{\pi}{a}$ (with a the lattice spacing). Moreover, the appearance of a sharp feature in the pair momentum distribution, as shown in Fig. 1, serves as a signature for the formation of spatially extended coherence. In cold atom experiments, such pair momentum distributions can be observed by the projection of the local pairs onto molecules [10, 11]. As our proposal relies both on dissipation and kinetic processes, it is conceptually very different from previous approaches where the η-pairing state was stabilized through either adiabatic state preparation [9, 12], or the imprint of phase coherence between neighboring sites by a tailored environment [4, 13].

II. INTERPLAY OF UNITARY AND DISSIPATIVE DYNAMICS

The system under consideration here is made of repulsively interacting fermions on a d-dimensional lattice of volume V and lattice constant a. We describe this many-body system by the Hubbard model

$$H = -J \sum_{\langle \mathbf{r}, \mathbf{r}' \rangle, \sigma} \left(\hat{c}^\dagger_{\mathbf{r},\sigma} \hat{c}_{\mathbf{r}',\sigma} + \text{h.c.} \right) + U \sum_{\mathbf{r}} \hat{n}_{\mathbf{r},\uparrow} \hat{n}_{\mathbf{r},\downarrow} \,,$$

where $\hat{c}^\dagger_{\mathbf{r},\sigma}$ is the creation operator for a fermion with spin $\sigma = \uparrow, \downarrow$ and site index $\mathbf{r}$, $\hat{n}_{\mathbf{r},\sigma} = \hat{c}^\dagger_{\mathbf{r},\sigma} \hat{c}_{\mathbf{r},\sigma}$ is the density operator, $J > 0$ is the hopping coefficient, U the interaction strength, and $\langle \mathbf{r}, \mathbf{r}' \rangle$ indicates that the sum is done over nearest-neighbors. This Hamiltonian is one of the simplest models capturing the interplay between the kinetic and interaction energies, and can be used, for example, to understand the metal to Mott insulator transition. A particularly clean realization of this model is achieved using ultracold fermionic gases confined to optical lattices [14].

In the present work, we assume the system to be initially prepared in a stationary state of this Hamiltonian, typically a Mott insulator as realized in Refs. [15, 16]. We study the system dynamics after coupling a dissipative environment to the local spin densities such that

$$\frac{d}{dt} \hat{\rho}(t) = -\frac{i}{\hbar} \big[\hat{H}, \hat{\rho}(t) \big] + \mathcal{D} \left[\hat{\rho}\,(t) \right] \,, \tag{1}$$

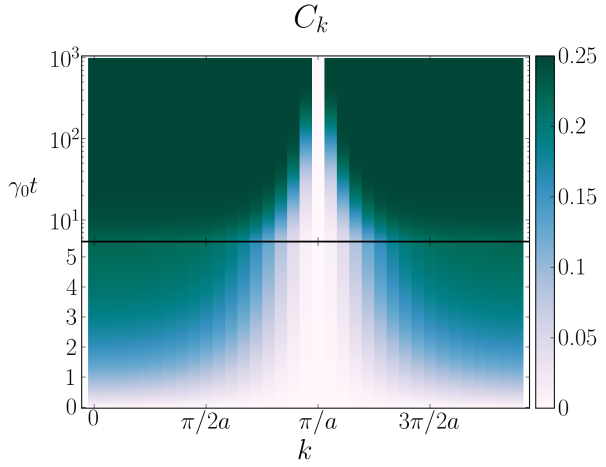

FIG. 1: (Color online) Time evolution of the momentum distribution of local pairs: $C_{\mathbf{k}} = \frac{1}{V}\sum_{\mathbf{r},\mathbf{d}} e^{-i a \mathbf{k}\cdot\mathbf{d}} \langle \hat{c}^\dagger_{\mathbf{r}\downarrow}\hat{c}^\dagger_{\mathbf{r}+\mathbf{d}\uparrow}\hat{c}_{\mathbf{r}+\mathbf{d}\uparrow}\hat{c}_{\mathbf{r}+\mathbf{d}\downarrow}\rangle$. A chain of $L = 36$ lattice sites is prepared at $t = 0$ in a perfect Mott insulating state where pair correlations are absent. A fast build-up in occupation of the momenta except close to $k = \frac{\pi}{a}$ takes place at short times (plotted on a linear time scale). Then, over time, all momenta except $k = \frac{\pi}{a}$ become homogeneously occupied, signaling the generation of the coherence of pairs over longer distances (plotted on a logarithmic scale). The evolution is obtained using the effective diffusion equation (3) with $\frac{U}{\hbar\Gamma} = 1.5$ and $\gamma_0 = \frac{8J^2}{\hbar^2\Gamma}$.

with

$$\mathcal{D}\left[\hat{\rho}(t)\right] = \Gamma \sum_{\mathbf{r}} \left(\hat{n}_{s,\mathbf{r}}\hat{\rho}\,\hat{n}_{s,\mathbf{r}} - \frac{1}{2}\hat{n}^2_{s,\mathbf{r}}\,\hat{\rho} - \frac{1}{2}\hat{\rho}\,\hat{n}^2_{s,\mathbf{r}} \right) . \quad (2)$$

The quantum jump operators $\hat{n}_{s,\mathbf{r}} = \hat{n}_{\uparrow,\mathbf{r}} - \hat{n}_{\downarrow,\mathbf{r}}$ measure the local spin polarization. The dissipative coupling $\mathcal{D}$ can be realized, for example, by a light field whose frequency is chosen in between the transitions of the two fermionic states as used for phase contrast imaging [7]. This light field can either be used to probe the spin density locally, e.g. in combination with an independent addressing of each site [17, 18] or to create "magnetic field" noise, e.g. through the realization of spatially-disordered and time-decorrelated white noise patterns.

This dissipative mechanism leads to an exponential decay of single particle correlations as $\langle \hat{c}^\dagger_{\mathbf{r},\sigma}\hat{c}_{\mathbf{r}+\mathbf{d},\sigma}\rangle \propto e^{-\Gamma t}$. In contrast, pair correlations $C_{\mathbf{d}} = \frac{1}{V}\sum_{\mathbf{r}} \langle \hat{c}^\dagger_{\mathbf{r}\downarrow}\hat{c}^\dagger_{\mathbf{r}+\mathbf{d}\uparrow}\hat{c}_{\mathbf{r}+\mathbf{d}\uparrow}\hat{c}_{\mathbf{r}+\mathbf{d}\downarrow}\rangle$, remain unchanged under the action of the dissipator, $\mathcal{D}$, as doublons (doubly occupied sites) and holes (empty sites), which have no net polarization, belong to the dissipation-free subspace. In particular, the η-paired state, generated through the repeated application of the operator $\hat{\eta}^\dagger = \sum_{\mathbf{r}} e^{i\boldsymbol{\pi}\cdot\mathbf{r}}\,\hat{c}^\dagger_{\mathbf{r}\uparrow}\hat{c}^\dagger_{\mathbf{r}\downarrow}$ on the vacuum, is part of this subspace; here $\boldsymbol{\pi} = (\pi, \ldots, \pi)$. As the η-paired state is an eigenstate of the Hamiltonian, it is immune against the action of both the unitary and dissipative operators (see Eq. (1)). In fact, the evolution of the system is constrained by the constant of motion $F = C_{\mathbf{k}=\pi/a}$, where $C_{\mathbf{k}} = \sum_{\mathbf{d}} e^{-i a \mathbf{k}\cdot\mathbf{d}}\, C_{\mathbf{d}}$ is the momentum distribution of the local pairs (Fig. 1). This constant of motion is proportional to the number of η-pairs, $\langle \hat{\eta}^\dagger\hat{\eta}\rangle$, initially present in the system. Interestingly, even if the initial state does not overlap with the η-paired state (the extreme case considered here), metastable correlations may emerge due to kinetic processes.

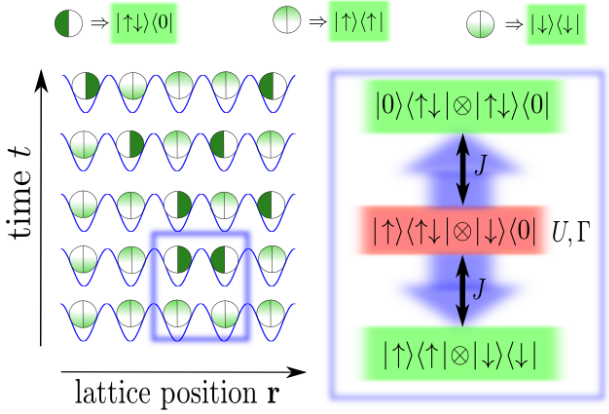

FIG. 2: (Color online) Left: Example of the effective creation and diffusion of pair correlations. The system evolution is described here using a locally factorized representation of the density matrix: each shaded circle corresponds to a local element of this density matrix. Right: Within the adiabatic elimination method, the evolution is based on the effective coupling of two states (lower and upper state) of the decoherence free subspace via a virtual excitation (center). The virtual state is reached by the hopping process and can decay with Γ and dephase due to interaction U. Here this process is examplified for a state with no pair correlations (lower state) connected to a state containing pair correlations (upper state) through the creation process (box) presented on the left panel.

III. EFFECTIVE DIFFUSION EQUATIONS

Irrespective of the coupling strength and the properties of the Hamiltonian, at sufficiently large times, $\Gamma t \gg 1$, the dissipation free subspace is reached. This subspace is highly degenerate with respect to the dissipator $\mathcal{D}$ and the Hamiltonian can lift this degeneracy. To understand the dynamics, we perform adiabatic elimination (see Supplemental Material) revealing how hopping-induced virtual excitations, around the dissipation-free subspace, affect the evolution of the system (cf. Fig. 2). The effective coupling via the virtual excitations depends on whether the interaction energy is changed during the process and takes the form

$$\gamma_0 = \frac{8J^2}{\hbar^2\Gamma} \quad \text{and} \quad \gamma_U = \frac{8J^2\Gamma}{\hbar^2\Gamma^2 + U^2} .$$

Using this perturbative approach, the equations describing the evolution of staggered pair correlations,

i.e. $\tilde{C}_{\mathbf{d}} = -e^{i\boldsymbol{\pi}\cdot\mathbf{d}} C_{\mathbf{d}} + \frac{\delta_{\mathbf{d},0}}{4}$, for times larger than $\frac{1}{\Gamma}$ are cast into a system of coupled diffusion equations (cf. Fig. 2, left panel):

$$\frac{d}{dt}\tilde{C}_{\mathbf{d}}(t) = \sum_{\mathbf{d}',\,|\mathbf{d}-\mathbf{d}'|=1} A_{\mathbf{d}',\mathbf{d}}(t)\left(\tilde{C}_{\mathbf{d}'}(t) - \tilde{C}_{\mathbf{d}}(t)\right). \qquad (3)$$

The diffusion constant depends on the coupling to the different virtual excitations weighted by their probability to occur,

$$A_{\mathbf{d}',\mathbf{d}}(t) \equiv D(t) = \gamma_0\left(\frac{1}{4} + \tilde{C}_0(t)\right) + \gamma_U\left(\frac{1}{4} - \tilde{C}_0(t)\right)$$

for $|\mathbf{d}|$ and $|\mathbf{d}'| \neq 0$, while $A_{\mathbf{d}',\mathbf{0}}(t) = A_{\mathbf{0},\mathbf{d}}(t) = \frac{\gamma_U}{2}$. For the sake of concreteness, we assumed above that the system was half filled and translationally invariant. Generalizations are straightforward and do not lead to qualitative changes. Moreover, we provide numerical evidence that this diffusive behavior is not restricted to the domain $\Gamma \gg \frac{J}{\hbar}$, but is valid even at weak coupling $\Gamma < \frac{J}{\hbar}$. However, in the latter case, the diffusion constant deviates from the perturbative results.

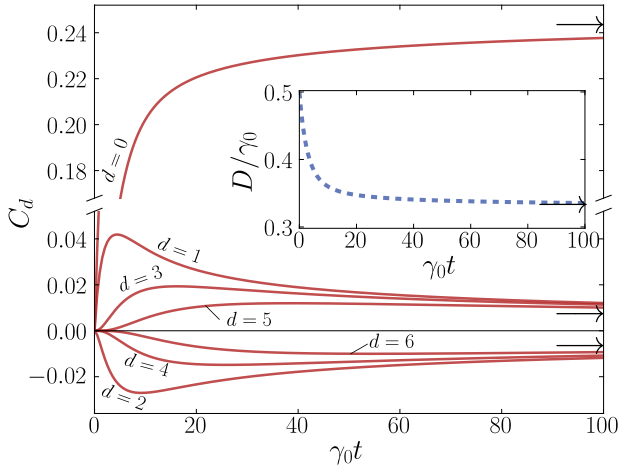

FIG. 3: (Color online) $C_d(t)$ as a function of time t as described by the diffusion equation (3). The chain is prepared in a perfect Mott insulator with $L = 36$ sites and evolves with $\frac{U}{\hbar\Gamma} = 1.5$. Arrows mark the $t \to \infty$ limit. The double occupancy, $C_{d=0}$, and nearest-neighbor pair correlation, $C_{d=1}$, raise quickly and feed the delayed increase of correlations at large distances. Inset: evolution of the diffusion constant as a function of time. $D(t)$ becomes time-independent as the double occupancy, $C_{d=0}$, saturates.

IV. CREATION OF METASTABLE PAIR CORRELATIONS

We illustrate the creation of correlations using, as an example, a system initially in a Mott insulating state, i.e. $C_{\mathbf{d}}(0) = 0$ for all $\mathbf{d}$. In Fig. 3 we depict the dynamics triggered by the action of the Hamiltonian, $\hat{H}$, and

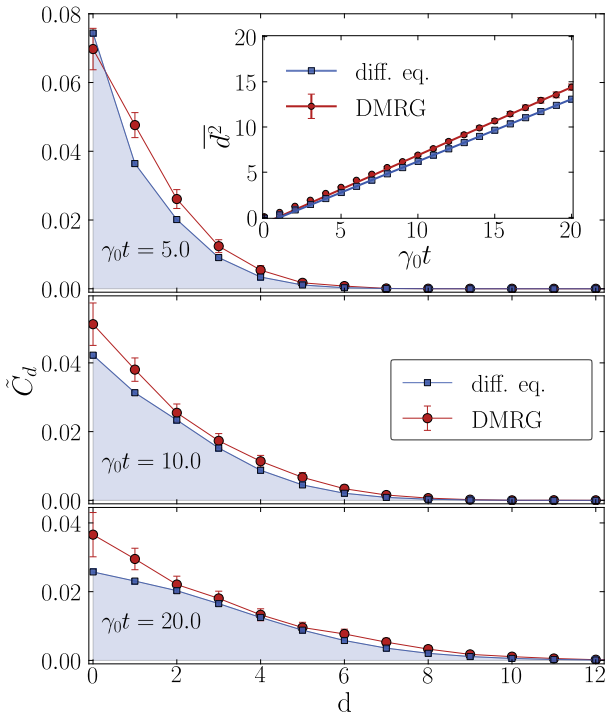

FIG. 4: (Color online) $\tilde{C}_d(t)$, the staggered pair correlations, are shown as a function of distance, d, for three different times in a chain of $L = 36$. We compare the solution of the diffusion equation (3) with time-dependent DMRG simulations. For both cases the initial conditions are taken from ground state DMRG calculations at $U = 12J$. We use $\frac{U}{\hbar\Gamma} = 1.5$ and in the time-dependent DMRG $U = 12J$. Inset: Symbols represent the variance of the pair correlation distribution versus time. Lines are linear fits for $10 < \gamma_0 t < 20$.

the dissipator, $\mathcal{D}$, on a one-dimensional system. First, double occupancy and short range pair correlations rise on the time scale $\frac{1}{\gamma_0}$. Then, following this initial build-up, the double occupancy and the nearest-neighbor pair correlation act as sources for the propagation of pair correlations over longer distances. Within the perturbatively derived Eq. (3), one expects the propagation of the staggered pair correlations to be described by a normal diffusion process. For an atomic Mott insulator, $\langle\hat{\eta}^\dagger\hat{\eta}\rangle = 0$. The pair correlations asymptotic values are uniquely determined by the initial state and are equal to $C_{\mathbf{d}}(t \to \infty) = -e^{i\boldsymbol{\pi}\cdot\mathbf{d}}\frac{1}{4V}$ for $|\mathbf{d}| \neq 0$ and $C_0(t \to \infty) = \frac{1}{4}\left(1 - \frac{1}{V}\right)$. While $C_{\mathbf{d}\neq 0}(t \to \infty) \to 0$ in the thermodynamical limit, it is essential to note that the metastable correlations are independent of the system size.

The "overall" sign of $C_{\mathbf{d}\neq 0}$, and thus the phase slip between $d = 0$ and $d = 1$ depends on the initial state and would differ if $F > \frac{1}{4}$ [19]. We note that the saturation of the double occupancy implies that the diffusion constant becomes time-independent: $D(t \to \infty) \sim \frac{\gamma_0+\gamma_U}{4}$ (see inset in Fig. 3). To study this diffusive spreading, we plot in Fig. 4 the staggered correlations at different

times versus distance. In terms of $\tilde{C}_{\mathbf{d}}$, the initial Mott insulator is characterized by a peak at $\mathbf{d} = 0$. As shown on Fig. 4, the interplay of dissipation and hopping gradually transforms this peak into a broad gaussian distribution.

To check the validity of our perturbative results against unbiased methods, we use time-dependent DMRG to solve the master equation (1) stochastically [20]. One can appreciate in Fig. 4 that the pair correlations obtained from DMRG are in good agreement with the pertubative results. Deviations away from the expected gaussian distribution mostly occur at short distances. This discrepancy is partially attributed to the decoupling of density correlations applied in the derivation of Eq. (3).

The diffusive propagation is best characterized by the variance

$$\overline{\mathbf{d}^2(t)} = \sum_{\mathbf{d}} \mathbf{d}^2 \tilde{C}_{\mathbf{d}}(t) / \sum_{\mathbf{d}} \tilde{C}_{\mathbf{d}}(0)\,.$$

Generally, for a hypercubic lattice with connectivity z, the variance of a diffusive process obeys

$$\frac{d}{dt}\overline{\mathbf{d}^2(t)} = zD(t)\,.$$

Within the perturbative treatment, at $t \gg \frac{1}{\gamma_0}$ where $D(t)$ becomes constant, the variance should rise linearly with time. The variance, shown in the inset of Fig. 4 confirms this statement. Small deviations from the linear behavior are consistent with the time-dependence of $D(t)$.

Remarkably, we find the diffusive description of the propagation of pair correlations to remain valid down to the weakly dissipative regime. However, in this regime, the diffusion constants need to be phenomenologically determined. In Fig. 5, we study a strongly interacting system $U = 12J$ with couplings from $\Gamma = 4\frac{J}{\hbar}$ down to $\Gamma = 0.25\frac{J}{\hbar}$. In all cases, a normal diffusive regime is entered after $t \sim \frac{1}{\Gamma}$. As shown in the inset of Fig. 5, the effective diffusion constants, in the strong dissipative coupling limit, agree nicely with our perturbative predictions. As expected, with decreasing Γ, the deviation from the analytic predictions increases. Nevertheless, the correct qualitative behavior is predicted for $\Gamma \gtrsim \frac{J}{\hbar}$: the effective diffusion constant increases with $\frac{1}{\Gamma}$. For $\Gamma \lesssim \frac{J}{\hbar}$ our simulations suggest a saturation of the diffusion constant to roughly $0.7\frac{J}{\hbar}$.

V. EXPERIMENTAL REALIZATION

Realizing this model and detecting pair correlations is within experimental reach. As explained earlier, the required dissipative coupling can be realized by a light field whose frequency is between the transitions of the two fermionic states as used in phase constrast imaging [7]. Probing the resulting pair coherence, visible for example in the pair momentum distribution, is also experimentally feasible. In fact, the detection of the pair momentum distribution has been achieved in another context

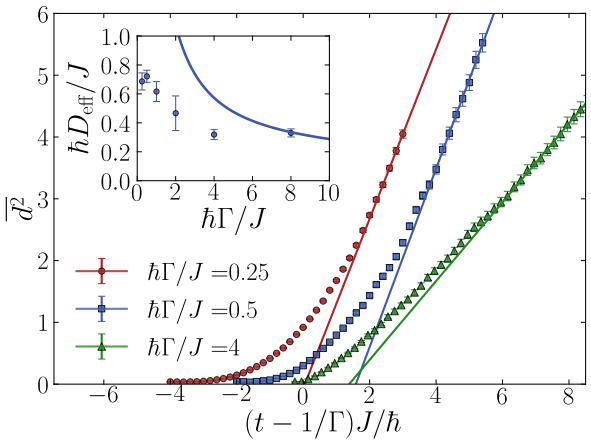

FIG. 5: (Color online) The variance of the distribution of the staggered pair correlations $\tilde{C}_d(t)$ with distance for different dissipative strength $\frac{\hbar\Gamma}{J}$ at constant $U = 12J$ in a chain of length 36. The linear rise of the variance at larger times is in accordance with a diffusive formation of the pair correlations. Symbols are taken from DMRG simulations, straight lines are linear fits $\overline{d^2} = 2D_{\rm eff}\,t + \text{const.}$ for values with $\overline{d^2} > 2.5$. Inset: $D_{\rm eff}$ as a function of dissipative coupling at $U = 12J$ (symbols). The straight line corresponds to $D(t \to \infty)$ derived within perturbation theory and agrees well with the numerical results for large coupling strengths.

by projecting local pairs onto molecules using an interaction ramp across a Feshbach resonance [10, 11]. A similar approach can be used here as the generation of correlations results in the formation of a sharp dip in the pair momentum distribution at $\mathbf{k} = \frac{\boldsymbol{\pi}}{a}$. To estimate the signal strength, we consider an experimentally realistic half filled one-dimensional chain of 36 lattice sites as shown in Fig. 1. From our calculations, we estimate that approximately one quarter of all atoms contribute to the pair momentum distribution. To detect pair formation, we propose to measure the contrast $\nu = \frac{C_{\mathbf{k}} - C_{\mathbf{k}=\boldsymbol{\pi}/a}}{C_{\mathbf{k}} + C_{\mathbf{k}=\boldsymbol{\pi}/a}}$ between the dip at $\mathbf{k} = \frac{\boldsymbol{\pi}}{a}$ and the constant background at the other momenta. ν will tend to one with increasing time. Experimentalists will be faced with two obvious challenges: the signal at each momentum (except for $\mathbf{k} = \frac{\boldsymbol{\pi}}{a}$) is of the order of a quarter of a single atom, and the dip might be difficult to resolve at large times due to its sharpness. Fortunately, we expect that both challenges can be overcome. As current experiments are routinely conducted in parallel on arrays of tubes (1d) or planes (2d), the detectable signal can be considerably enhanced [21]. Also, the dip can be measured at intermediate times (in the metastable regime) when it still covers approximately $\frac{1}{8}$ of the Brillouin zone.

VI. CONCLUSION

In summary, we demonstrated here that the combined action of incoherent local environmental coupling and ki-

netic processes can result in the emergence of metastable spatially extended pair correlations in repulsive fermionic lattice systems. In contrast to correlations realized in cooled condensed matter systems, typically sensitive to temperature, the non-equilibrium mechanism presented above is immune against thermal fluctuations. This conceptually surprising approach provides a new route towards a better control of quantum many-body correlations.

Acknowledgments

We thank E. Demler, T. Esslinger, V. Galitski, A. Kantian, M. Köhl, H. Pichler, A. Rosch and P. Zoller for fruitful discussions, and A. Georges for his valuable contributions to the early part of this work. Our computer simulations employed the ALPS libraries [22–25]. We acknowledge ANR (FAMOUS), SNSF under Division II, MaNEP, CIFAR and NSERC for their financial support and the KITP (grant no. NSF PHY11-25915) for its hospitality.

Appendix A: Adiabatic elimination

Locally, the dissipation free subspace with respect to $\mathcal{D}$ is spanned by the diagonal operators $\{\hat{p}_{\mathbf{r},0} = |0\rangle\langle 0|, \hat{p}_{\mathbf{r},\downarrow} = |\downarrow\rangle\langle\downarrow|, \hat{p}_{\mathbf{r},\uparrow} = |\uparrow\rangle\langle\uparrow|, \hat{p}_{\mathbf{r},\uparrow\downarrow} = |\uparrow\downarrow\rangle\langle\uparrow\downarrow|\}$, and the off-diagonal operators $\{\hat{d}_{\mathbf{r}} = |0\rangle\langle\uparrow\downarrow|, \hat{d}^\dagger_{\mathbf{r}} = |\uparrow\downarrow\rangle\langle 0|\}$ annihilating or creating a pair at site $\mathbf{r}$ such that $\hat{d}^\dagger_{\mathbf{r}} = \hat{c}^\dagger_{\mathbf{r}\uparrow}\hat{c}^\dagger_{\mathbf{r}\downarrow}$. In addition, the first excited subpace can be defined via the basis elements $\{\hat{p}_{\mathbf{r},0}\hat{c}_{\mathbf{r},\sigma}, \hat{c}^\dagger_{\mathbf{r},\sigma}\hat{p}_{\mathbf{r},0}, \hat{p}_{\mathbf{r},\downarrow\uparrow}\hat{c}^\dagger_{\mathbf{r},\sigma}, \hat{c}_{\mathbf{r},\sigma}\hat{p}_{\mathbf{r},\uparrow\downarrow}\}$. These operators form a diagonal basis for $-\frac{iU}{\hbar}\left[\hat{p}_{\mathbf{r},\uparrow\downarrow}, .\right] + \mathcal{D}\left[.\right]$ with eigenvalues $\lambda_\alpha \in \{-\frac{\Gamma}{2}, -\frac{\Gamma}{2}, -\frac{\Gamma}{2}+i\frac{U}{\hbar}, -\frac{\Gamma}{2}-i\frac{U}{\hbar}\}$, $\alpha = 1, \ldots, 4$. We associate a projector $\mathcal{P}^\alpha_{\mathbf{r}}$ to each subspace associated with a certain eigenvalue of the excited subspace, while $\mathcal{P}^0_{\mathbf{r}}$ projects onto the dissipation free subspace. Via adiabatic elimination of the excited subspace (see e.g. [26]), one derives effective equations of motion for the basis elements within the dissipation free subspace, for example

$$\begin{aligned}\frac{d}{dt}\hat{d}_{\mathbf{r}} &= \sum_{\substack{\mathbf{r}',\,|\mathbf{r}-\mathbf{r}'|=1\\ \alpha,\alpha'=1,\ldots,4}} \frac{J^2}{\hbar^2}\frac{\mathcal{P}^0_{\mathbf{r}}\mathcal{P}^0_{\mathbf{r}'}\left[\hat{K}_{\mathbf{r},\mathbf{r}'}, \mathcal{P}^\alpha_{\mathbf{r}}\mathcal{P}^{\alpha'}_{\mathbf{r}'}\left[\hat{K}_{\mathbf{r},\mathbf{r}'}, \hat{d}_{\mathbf{r}}\right]\right]}{\lambda_\alpha + \lambda_{\alpha'} + i\frac{U}{\hbar}} \\ &= \sum_{\mathbf{r}',\,|\mathbf{r}-\mathbf{r}'|=1} \hat{A}_{\mathbf{r}'}\hat{d}_{\mathbf{r}} + \hat{A}_{\mathbf{r}}\hat{d}_{\mathbf{r}'}, \qquad \text{(A1)}\end{aligned}$$

$$\text{with } \hat{A}_{\mathbf{r}} = -2\frac{J^2}{\hbar^2}\left\{\frac{(\hat{p}_{\mathbf{r},\uparrow} + \hat{p}_{\mathbf{r},\downarrow})}{\Gamma} + \frac{\hat{p}_{\mathbf{r},\downarrow\uparrow}}{\Gamma + i\frac{U}{\hbar}} + \frac{\hat{p}_{\mathbf{r},0}}{\Gamma - i\frac{U}{\hbar}}\right\}$$

and $\hat{K}_{\mathbf{r},\mathbf{r}'} = \hat{c}^\dagger_{\mathbf{r},\sigma}\hat{c}_{\mathbf{r}',\sigma} + \text{h.c.}$ Eq. (A1) is used to derive the equation of motion for $\hat{d}^\dagger_{\mathbf{r}}\hat{d}_{\mathbf{r}'}$ with $|\mathbf{r}-\mathbf{r}'| > 1$. A similar procedure is used to find the equations for $|\mathbf{r}-\mathbf{r}'| \leq 1$. In order to construct the closed set of equations of motion for the pair correlators, Eq. (3), we decouple $\langle\hat{p}_{\mathbf{r},n}\hat{O}_{\mathbf{r}'}\rangle$ as $\langle\hat{p}_{\mathbf{r},n}\rangle\langle\hat{O}_{\mathbf{r}'}\rangle$ where $n = \{0, \uparrow, \downarrow, \uparrow\downarrow\}$ and $\hat{O}_{\mathbf{r}'}$ is an arbitrary local operator on site $\mathbf{r}' \neq \mathbf{r}$.

[1] D. N. Basov, R. D. Averitt, D. van der Marel, M. Dressel, and K. Haule, Rev. Mod. Phys., **83**, 471 (2011).
[2] K. W. Kim, A. Pashkin, H. Schäfer, M. Beyer, M. Porer, T. Wolf, C. Bernhard, J. Demsar, R. Huber, and A. Leitenstorfer, Nature Materials, **11**, 497 (2012).
[3] D. Fausti, R. I. Tobey, N. Dean, S. Kaiser, A. Dienst, M. C. Hoffmann, S. Pyon, T. Takayama, H. Takagi, and A. Cavalleri, Science, **331**, 189 (2011).
[4] M. Müller, S. Diehl, G. Pupillo, and P. Zoller, Advances in Atomic, Molecular, and Optical Physics, **61**, 1 (2012).
[5] J. Barreiro, M. Müller, P. Schindler, D. Nigg, T. Monz, M. Chwalla, M. Hennrich, C. Roos, P. Zoller, and R. Blatt, Nature, **470**, 486 (2011).
[6] D. M. Bauer, N. Syassen, D. Dietze, T. Volz, G. Rempe, J.-J. Garcia-Ripoll, J. I. Cirac, S. Dürr, and M. Lettner, "A dissipative Tonks-Girardeau gas of molecules," in *Pushing the frontiers of atomic physics* (World Scientific, Singapore, 2008) Chap. 29, pp. 307–314.
[7] Y. Shin, M. W. Zwierlein, C. H. Schunck, A. Schirotzek, and W. Ketterle, Phys. Rev. Lett., **97**, 030401 (2006).
[8] C. N. Yang, Phys. Rev. Lett., **63**, 2144 (1989).
[9] A. Rosch, D. Rasch, B. Binz, and M. Vojta, Phys. Rev. Lett., **101**, 265301 (2008).
[10] C. A. Regal, M. Greiner, and D. S. Jin, Phys. Rev. Lett., **92**, 040403 (2004).
[11] M. W. Zwierlein, C. A. Stan, C. H. Schunck, S. M. F. Raupach, A. J. Kerman, and W. Ketterle, Phys. Rev. Lett., **92**, 120403 (2004).
[12] A. Kantian, A. J. Daley, and P. Zoller, Phys. Rev. Lett., **104**, 240406 (2010).
[13] S. Diehl, A. Micheli, A. Kantian, B. Kraus, H. Büchler, and P. Zoller, Nature Physics, **4**, 878 (2008).
[14] M. Köhl, H. Moritz, T. Stöferle, K. Günter, and T. Esslinger, Phys. Rev. Lett., **94**, 080403 (2005).
[15] U. Schneider, L. Hackermüller, S. Will, T. Best, I. Bloch, T. A. Costi, R. W. Helmes, D. Rasch, and A. Rosch, Science, **322**, 1520 (2008).
[16] R. Jördens, N. Strohmaier, K. Günter, H. Moritz, and T. Esslinger, Nature, **455**, 204 (2008).
[17] W. S. Bakr, J. I. Gillen, A. Peng, S. Fölling, and M. Greiner, Nature, **462**, 74 (2009), ISSN 1476-4687.
[18] J. F. Sherson, C. Weitenberg, M. Endres, M. Cheneau, I. Bloch, and S. Kuhr, Nature, **467**, 68 (2010), ISSN 1476-4687.
[19] $C_{\mathbf{d}}(t \to \infty) = -\frac{1}{V}\, e^{i\boldsymbol{\pi}\cdot\mathbf{d}}\, (\frac{1}{4} - F) = -\, e^{i\boldsymbol{\pi}\cdot\mathbf{d}}\, (\frac{1}{4V} - \frac{1}{V^2}\langle\hat{\eta}^\dagger\hat{\eta}\rangle)$ for $|\mathbf{d}| \neq 0$.
[20] The timestep used in the integration via Suzuki-Trotter decomposition is about $0.02\frac{1}{\Gamma}$. Numerical accuracy was

ensured by retaining between 400 DMRG states (for $\frac{\hbar\Gamma}{J} = 8$) and 2500 states (for $\frac{\hbar\Gamma}{J} = 0.25$) and we typically sampled over a few thousand stochastic realizations.

[21] Let us note for completeness that a slightly inhomogeneous filling should not strongly affect the signal shape and strength.

[22] A.F. Albuquerque, F. Alet, P. Corboz, P. Dayal, A. Feiguin, S. Fuchs, L. Gamper, E. Gull, S. Gürtler, A. Honecker, R. Igarashi, M. Krner, A. Kozhevnikov, A. Läuchli, S.R. Manmana, M. Matsumoto, I.P. McCulloch, F. Michel, R.M. Noack, G. Pawlowski, L. Pollet, T. Pruschke, U. Schollwöck, S. Todo, S. Trebst, M. Troyer, P. Werner, and S. Wessel, J. of Magn. and Magn. Mat. **310**, 1187 (2007).

[23] A.B. Bauer, L.D. Carr, H.G. Evertz, A. Feiguin, J. Freire, S. Fuchs, L. Gamper, J. Gukelberger. E. Gull, S. Gürtler, A. Hehn, R. Igarashi, S.V. Isakov, D. Koop, P.N. Ma, P. Mates, H. Matsuo, O. Parcollet, G. Pawlowski, J.D. Picon, L. Pollet, E. Santos, V.W. Scarola, U. Schollwöck, C. Silva, B. Surer, S. Todo, S. Trebst, M. Troyer, M.L. Wall, P. Werner, and S. Wessel, J. Stat. Mech. (2011) P05001.

[24] M. Troyer, B. Ammon, and E. Heeb, Lect. Notes in Comp. Sci., **1505**, 191 (1998).

[25] http://alps.comp-phys.org

[26] J. J. García-Ripoll, S. Dürr, N. Syassen, D. M. Bauer, M. Lettner, G. Rempe, and J. I. Cirac, New Journal of Physics, **11**, 013053 (2009).